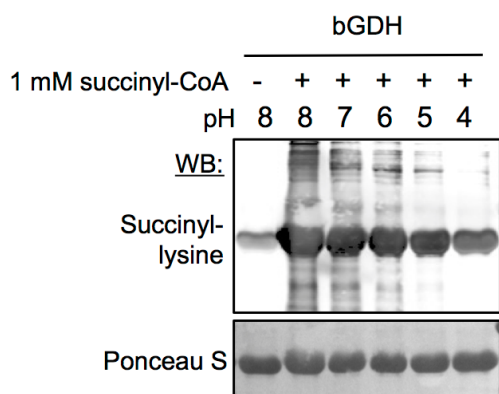
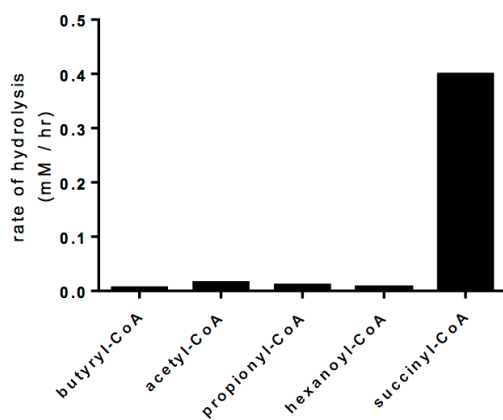
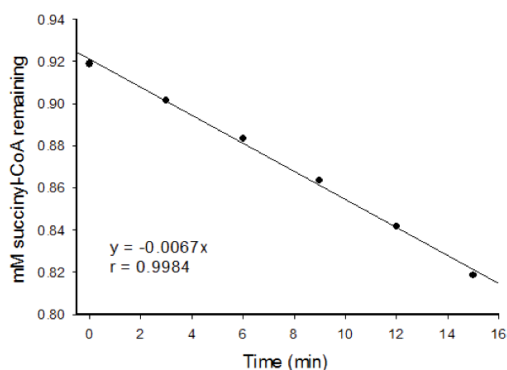


A**B****C****Zero Order**

$$T^{1/2} = [\text{Succinyl-CoA initial}] / (2 \cdot \text{rate})$$

$$T^{1/2} = [0.9188 \text{ mM}] / (2 \cdot 0.0067 \text{ mM / min})$$

$$T^{1/2} = 68.57 \text{ min} = 1.14 \text{ hr}$$

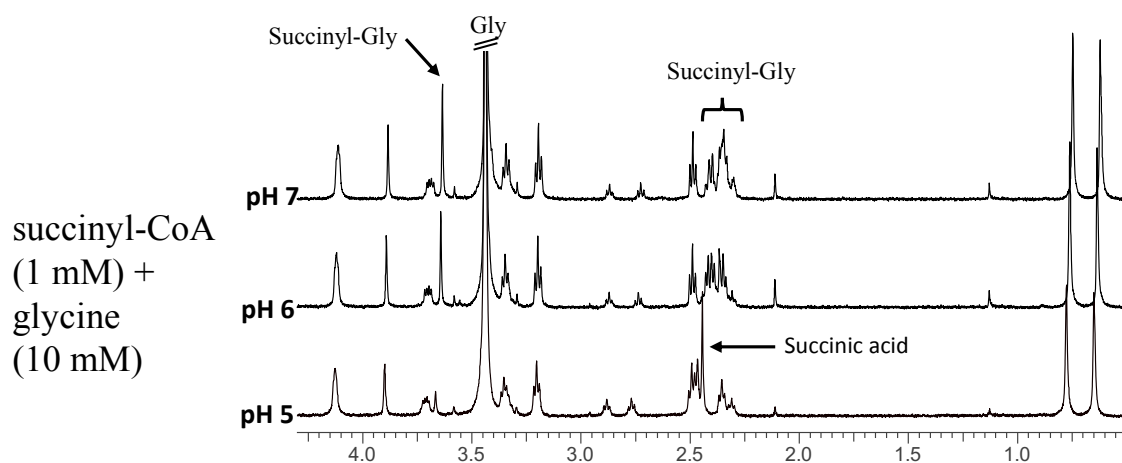
Figure S1, related to Figure 1. Succinyl-CoA is a highly efficient acylating agent.

(A) Succinyl-CoA acylates purified bovine glutamate dehydrogenase (bGDH) under acidic conditions similar to succinyl-CoA mediated succinylation of BSA, demonstrating acylation effect is not specific to the BSA substrate.

(B) Acyl-CoA hydrolysis rates in millimolar per hour (mM/hr) as measured by CoASH formation from 1 mM of each acyl-CoA. Rates were calculated from the slopes of the regression lines in primary Figure 2B.

(C) The kinetics of succinyl-CoA degradation at 25°C and pH 8.0 as monitored by CoASH formation. Over this time, the data was fitted to zero-order kinetic model, from which the half-life of succinyl-CoA was calculated to be 68.57 minutes. In (B) the nitrocellulose membranes used for immunoblotting were stained with the non-specific protein marker Ponceau S to show equal loading. WB, Western blot.

A



B

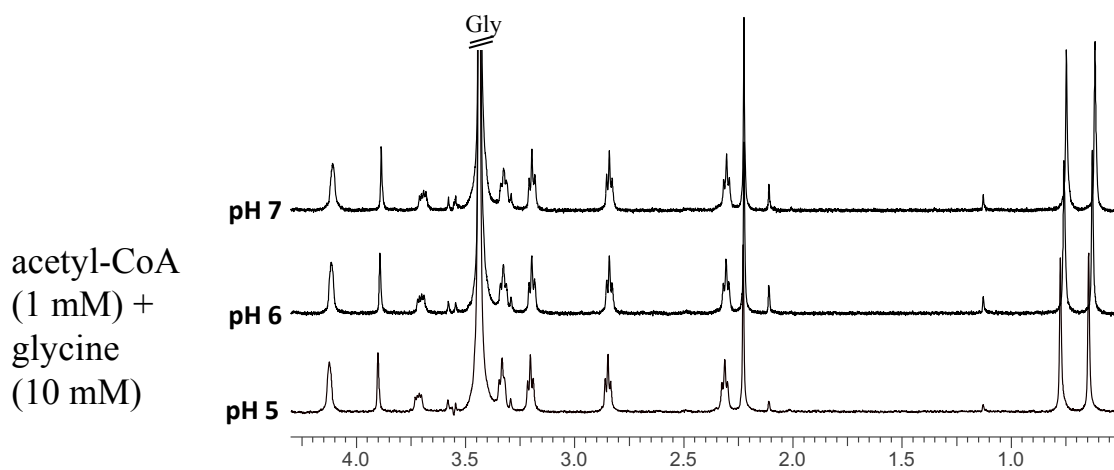


Figure S2, related to Figure 2. NMR spectra of succinyl-CoA plus glycine and acetyl-CoA plus glycine at pH 5, 6, and 7. Assay of pH conditions for acetyl-CoA and succinyl-CoA plus glycine to detect the formation of glycine adducts

(A) NMR spectra of succinyl-CoA plus glycine shows formation of the succinyl-glycine adduct starting at pH 5.0.

(B) NMR spectra of acetyl-CoA plus glycine shows no evidence of adduct formation across the pH range.

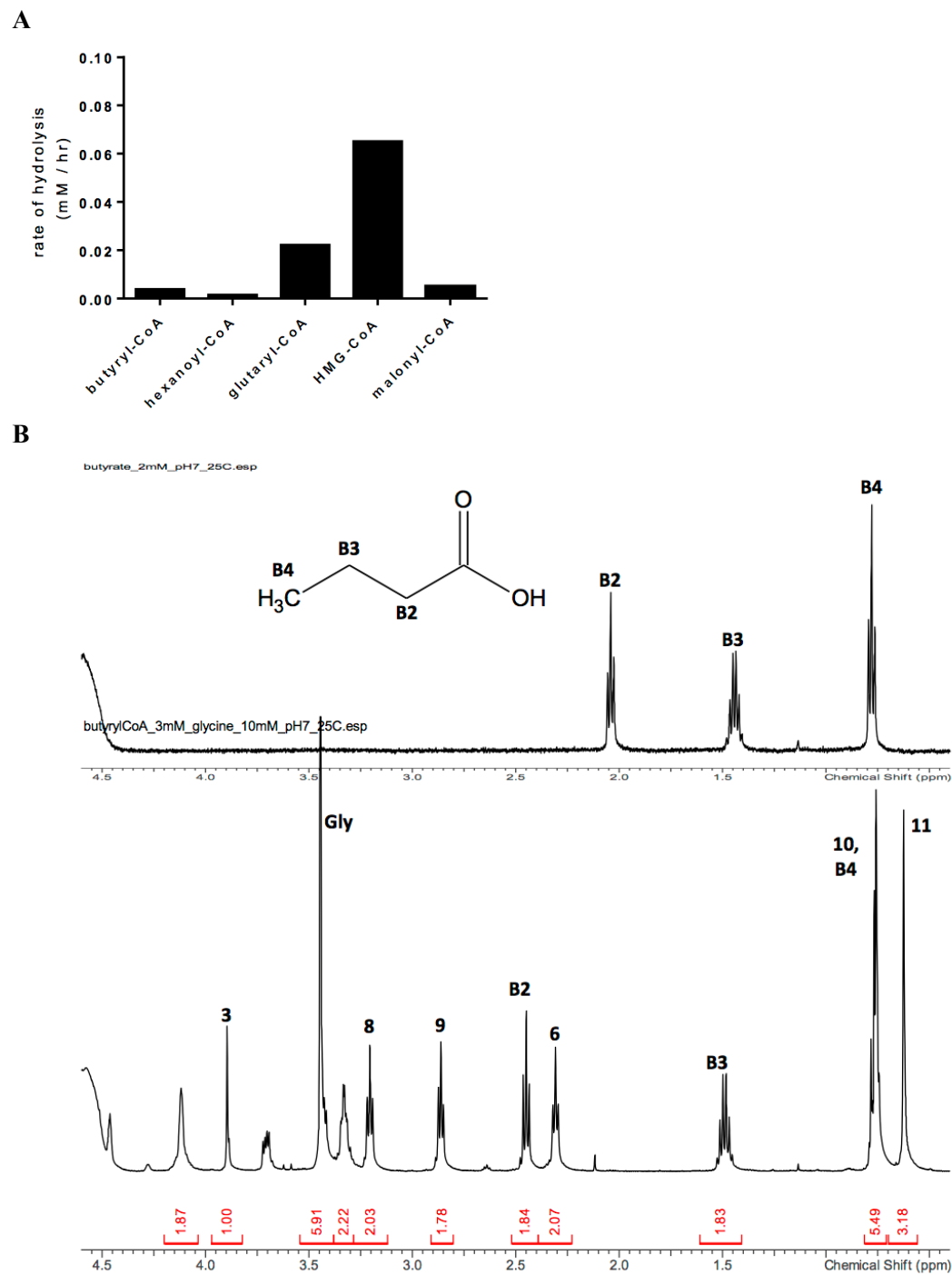


Figure S3, related to Figure 3.

(A) Acyl-CoA hydrolysis rates in millimolar per hour (mM/hr) as measured by CoASH formation from 1 mM of each acyl-CoA. Rates were calculated from the slopes of the regression lines in primary Figure 3A.

(B) NMR Spectra of Butyrate and Butyryl CoA + Glycine. The top spectrum shows the assignments for the butyric acid at pH 7 and below is butyryl CoA + glycine. The bottom spectrum shows the peaks shifts for the butyrate moiety when attached to the CoA. The lack of a significant singlet around 3.6 indicates that no butyrylglycine was formed.

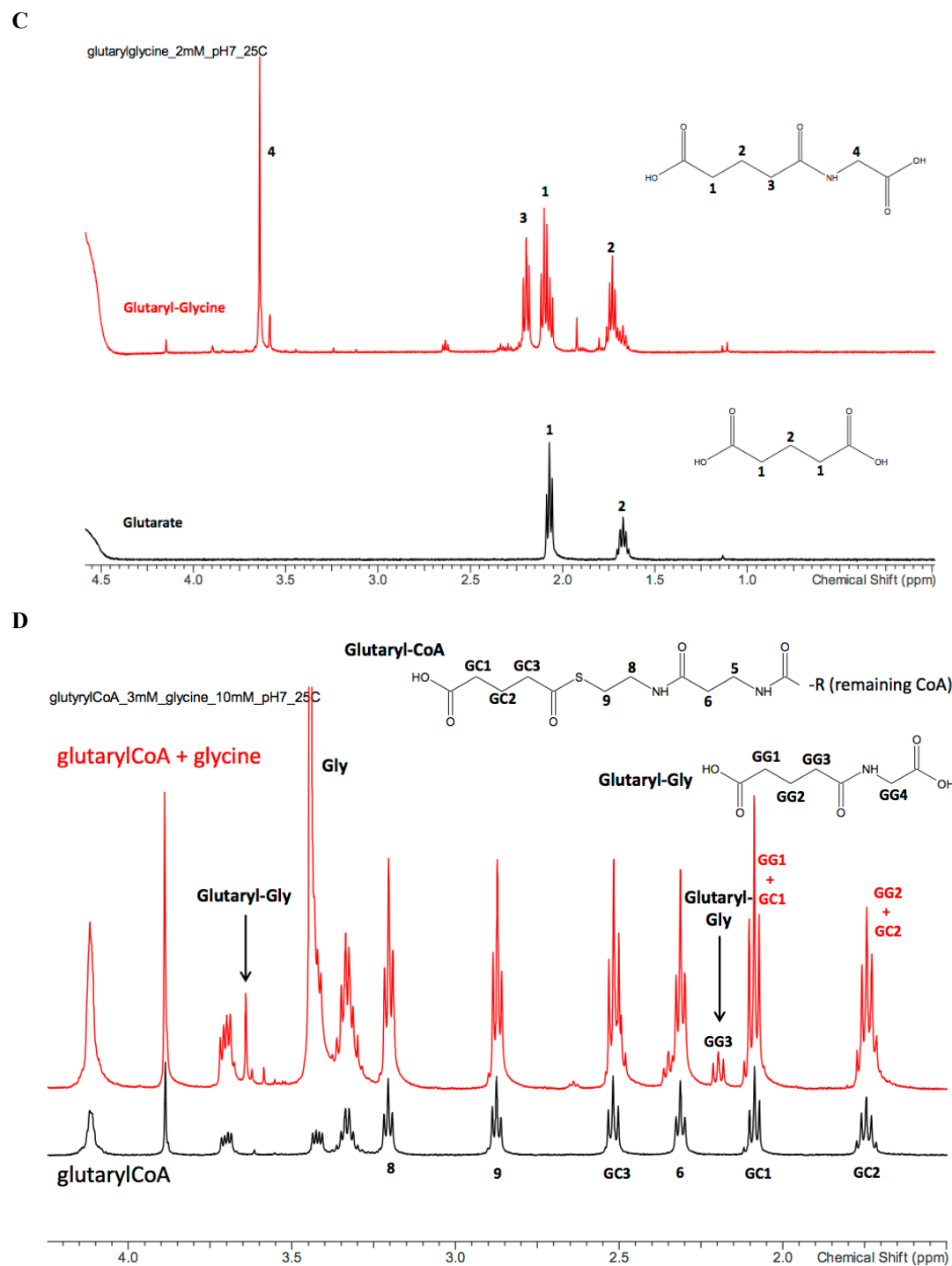
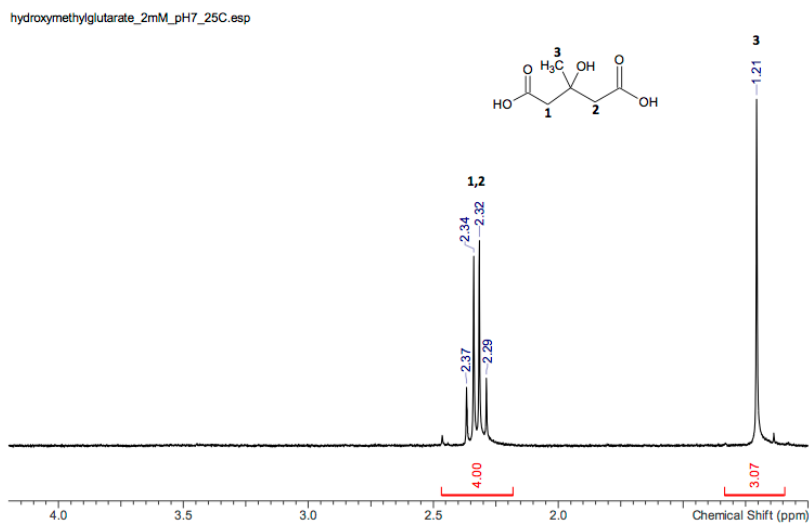
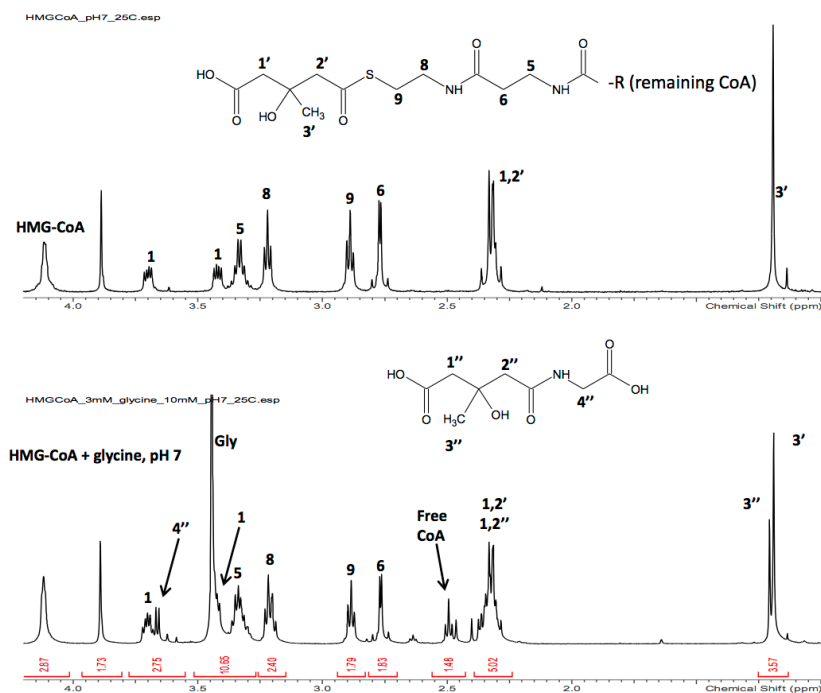


Figure S3, related to Figure 3, continued.

(C) NMR Spectra of Glutarate and Glutaryl-glycine. The top spectrum shows the assignments for a synthesized glutaryl-glycine at pH 7 (with obvious reaction impurities) and on the bottom glutarate.

(D) NMR Spectra of Glutaryl CoA and Glutaryl CoA + Glycine. The bottom spectrum is glutaryl-CoA alone. The GC1, GC2 and GC3 multiplets are assigned based on comparison with the acetyl and succinyl-CoA spectra. The GG1, 2 & 3 multiplets share consistent coupling which aided in the assignment of the 6 multiplet. The formation of glutaryl-glycine from the glutaryl-CoA + glycine is indicated by the methylene singlet at 3.64 ppm and the new GG3 triplet at 2.20 ppm. The GG1 and GG2 peaks appear to be overlapping with the glutaryl-CoA peaks.

E**F****Figure S3, related to Figure 3, continued.**

(E) NMR Spectra of hydroxymethylglutarate (HMG), pH 7, 25C. The HMG spectrum shows a singlet for the methyl group a multiplet that appears to be from a symmetric AB pattern. The AB pattern may stem from pseudochirality (acid groups are mirror images about the quaternary carbon).

(F) NMR Spectra of HMG-CoA and HMG-CoA + Glycine, pH 7, 25C. The top figure shows the HMG-CoA with annotations of the HMG appendage numbered with a single prime. The 1', 2' multiples remain an asymmetric AB pattern. The bottom figures show the HMG-CoA + glycine. The peaks for the HMG-glycine product are indicated by double primes. The 3'' methyl group is just downfield of the 3' methyl group from HMG-CoA. The 1, 2 multiples from both species are overlapping. This is confirmed by the large integral value of this region. The multiplet at 2.5 ppm matches the 6 proton from Acyl CoA and therefore may be this same proton on the free CoA that is released after formation of the HMG-Gly. The 4'' methylene group in other species e.g. succinyl-gly is a singlet, but due to the asymmetry imposed by the hydroxyl methyl substitution, this peak appears to be split.

G

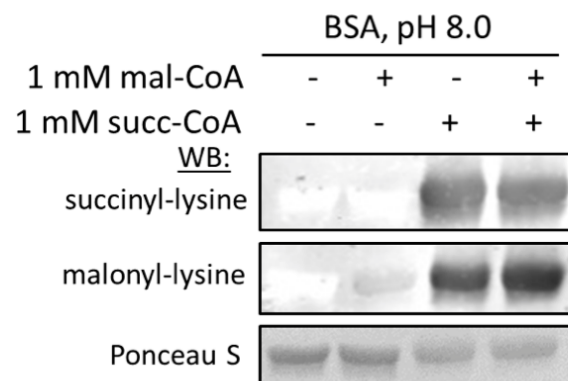


Figure S3, related to Figure 3, continued.

(G) Succinyl-CoA outcompetes malonyl-CoA for protein acylation as judged by the protein molecular mass shift induced only by succinyl-CoA and no loss in succinyl-lysine signal in the malonyl-CoA + succinyl-CoA co-treated condition. Due cross-reactivity of the malonyl-lysine antibody with succinyl-lysine modifications, substantial immunoreactive signal is observed in the succinyl-CoA treated conditions when using the malonyl-lysine antibody. Note the relatively minimal immunoreactive signal specific to malonyl-lysine modifications observed in the malonyl-CoA treated condition (lane 2).

A

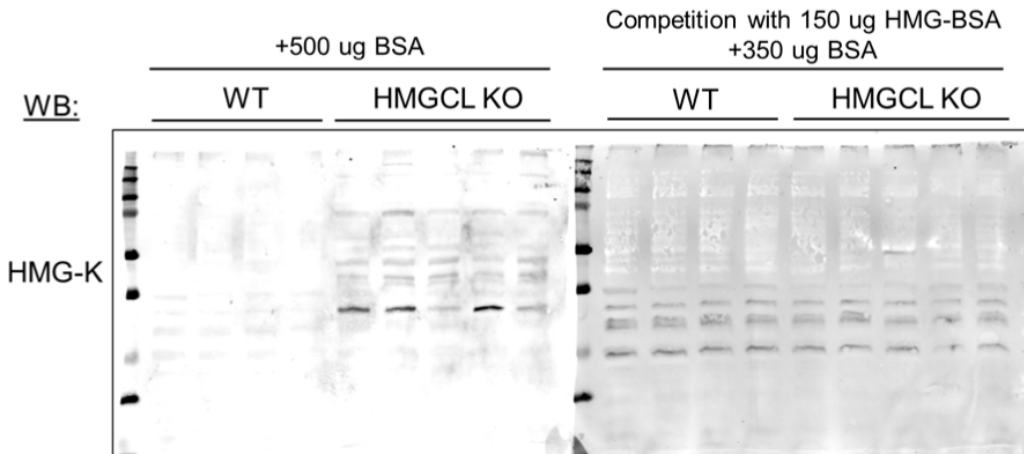
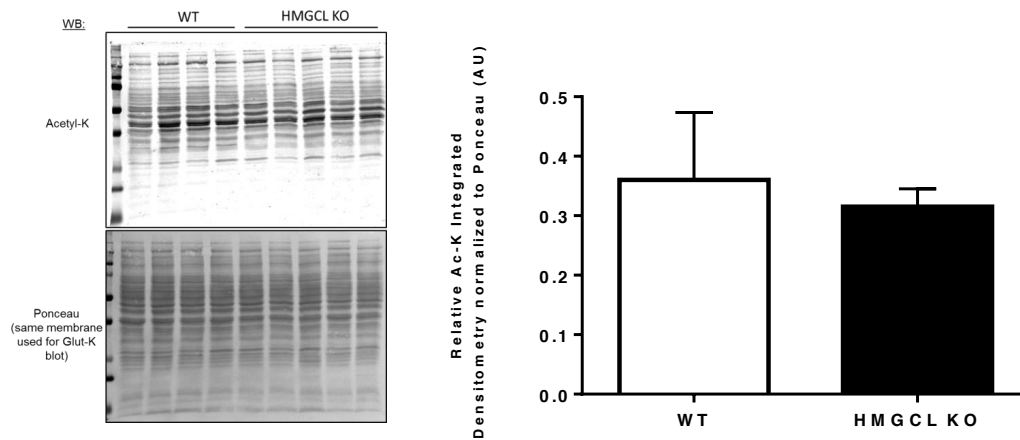
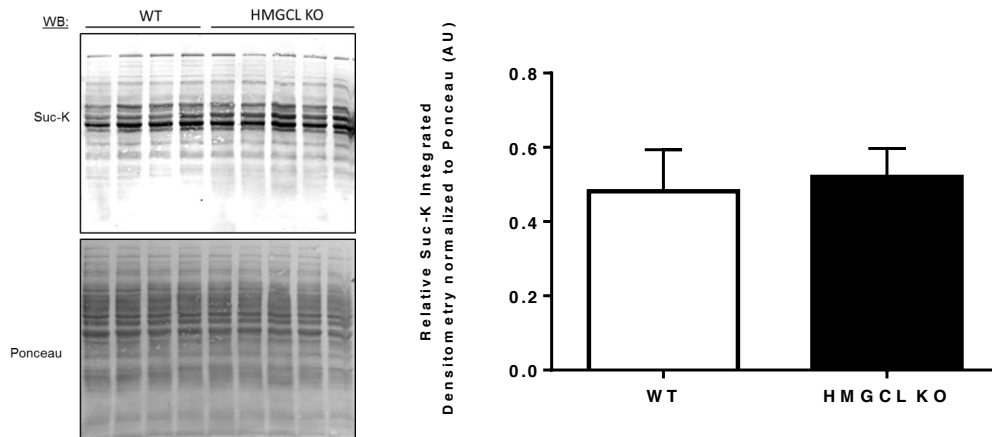
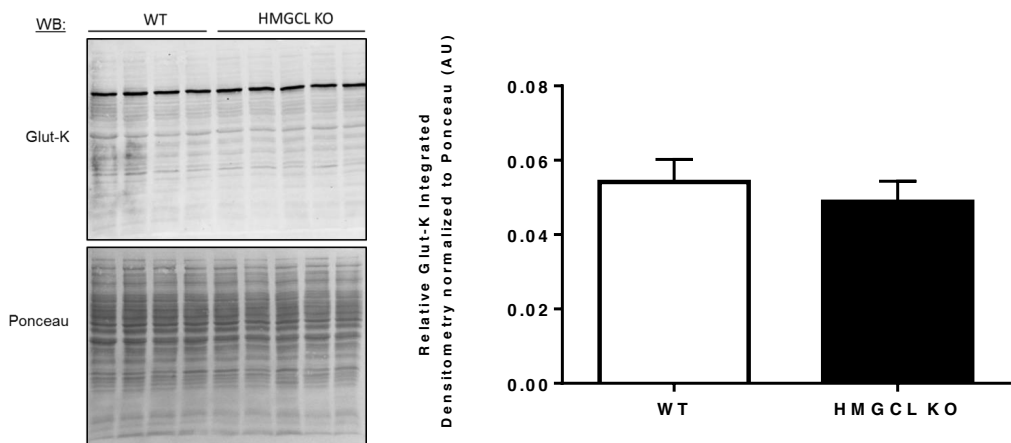


Figure S4, related to Figure 4.

(A) A single image of two Western blotting membranes containing the same amount of protein from WT (n=4) and HMGCL KO (n=5) livers and probed with an HMG-lysine antiserum during incubation with unmodified bovine serum albumin (left membrane) or during competition with chemically hydroxymethylglutarylated bovine serum albumin (right membrane) as indicated. BSA, bovine serum albumin. HMG-BSA, hydroxymethylglutarylated bovine serum albumin. WB, Western blot.

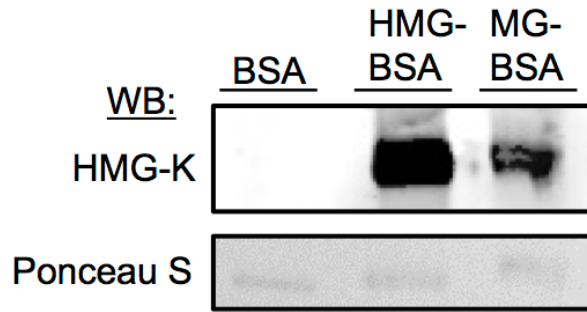
B**C****D****Figure S4, related to Figure 4, continued.**

(B) Western blot probing for protein lysine acetylation in liver lysates from wild-type (WT) (n=4) and HMGCL deficient mice (n=5). At right, the integrated densitometry of acetyl-lysine signal was quantified for each condition

(C) Similar to (A), only probing for protein lysine succinylation.

(D) Similar to (A), only probing for protein lysine glutarylation. The same membrane used to probe lysine acetylation in (A) was used to probe for lysine glutarylation. WB, Western blot. Data represent mean normalized to Ponceau S signal \pm standard deviation.

E



F

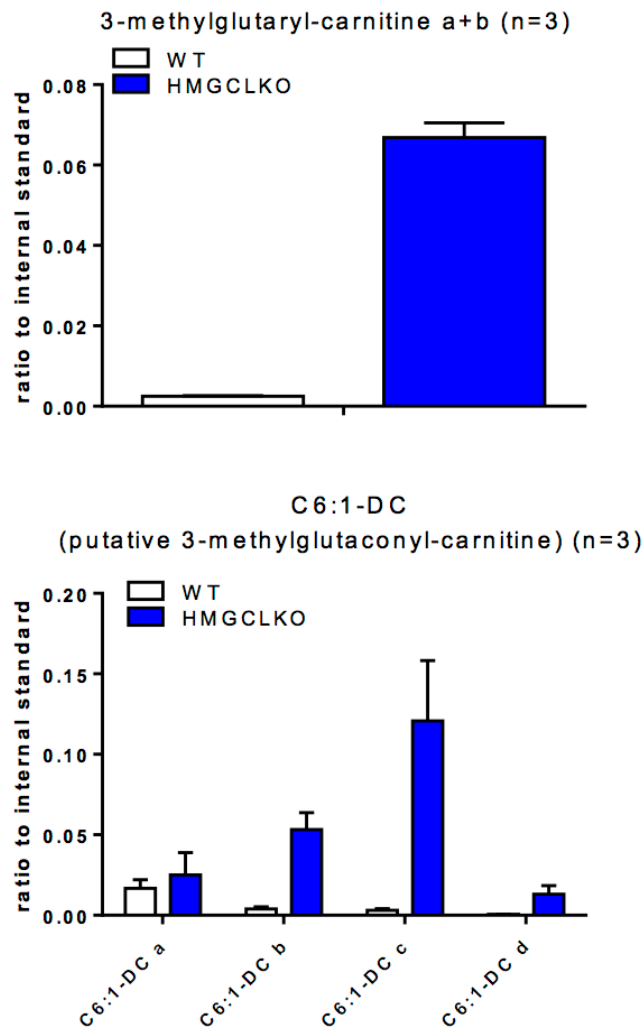
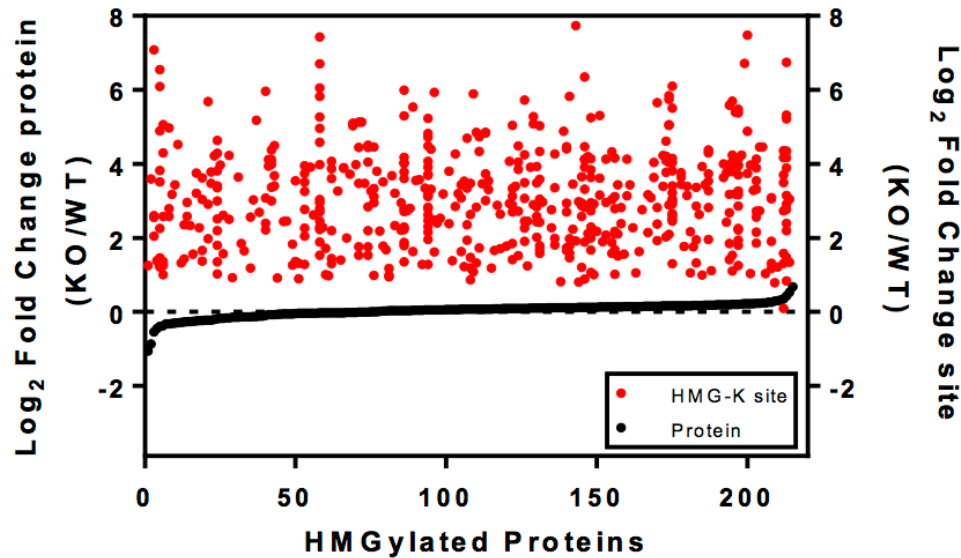


Figure S4, related to Figure 4, continued.

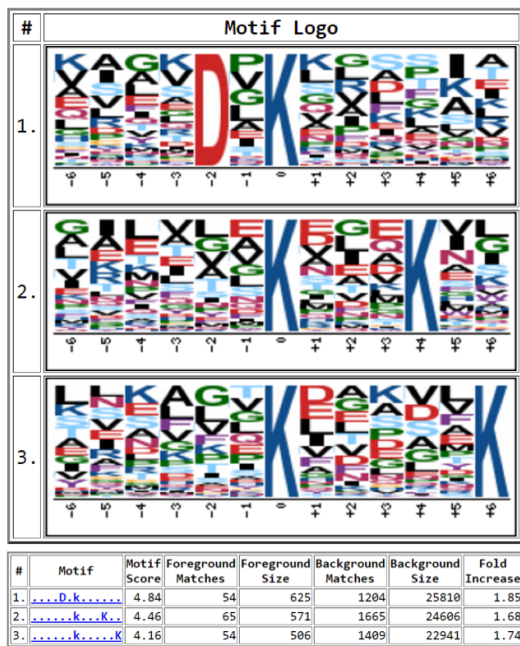
(E) Western blot demonstrating the HMG-lysine polyclonal antiserum cross-reacts with bovine serum albumin (BSA) chemically modified to contain 3-methylglutaryl-lysine (MG-K) modifications.

(F) The indicated acyl-carnitines were derivatized to butyl-esters and separated from their isomers via liquid chromatography followed by mass spectrometry. Data represent mean \pm standard deviation. WB, Western blot

A



B



C

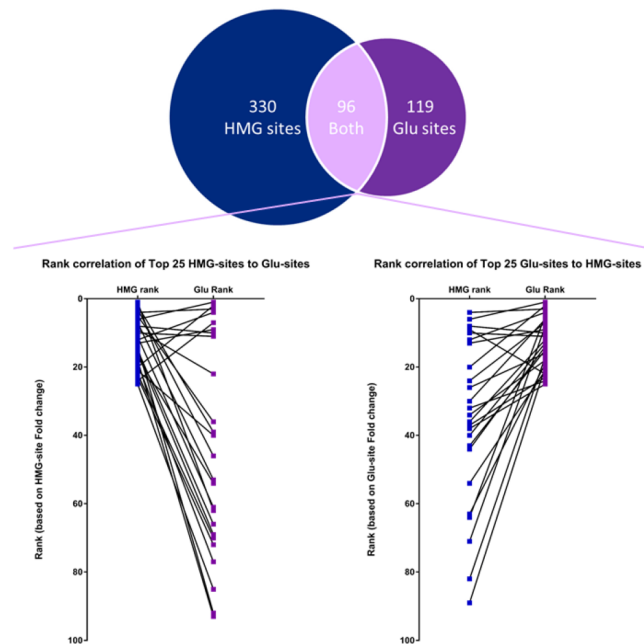


Figure S5, related to Figure 5.

(A) Fold change in HMGylation compared to fold change of the corresponding HMGylated proteins, both on the y-axis. Black dots represent the fold change in abundance of HMGylated proteins (quantitation from unmodified peptides in the “input” fraction only) in the HMGCL KO mitochondria relative to WT mitochondria, rank ordered from largest decrease to largest increase. Red dots represent the fold change in abundance of HMGylation (quantitation from HMGylated peptides in the IP eluate) at specific lysine residues within a given protein (corresponding protein at the same position on the x-axis).

(B) HMG-lysine motif analysis using motif-X. Summary of the motif-XF motif output including identified HMG-lysine motifs and the corresponding tables indicating the motif score and descriptive statistics.

(C) Rank correlation of top 25 protein acylation sites commonly modified by both HMGylation and glutarylation, and compared to the rank of the acylation site of the other modification.

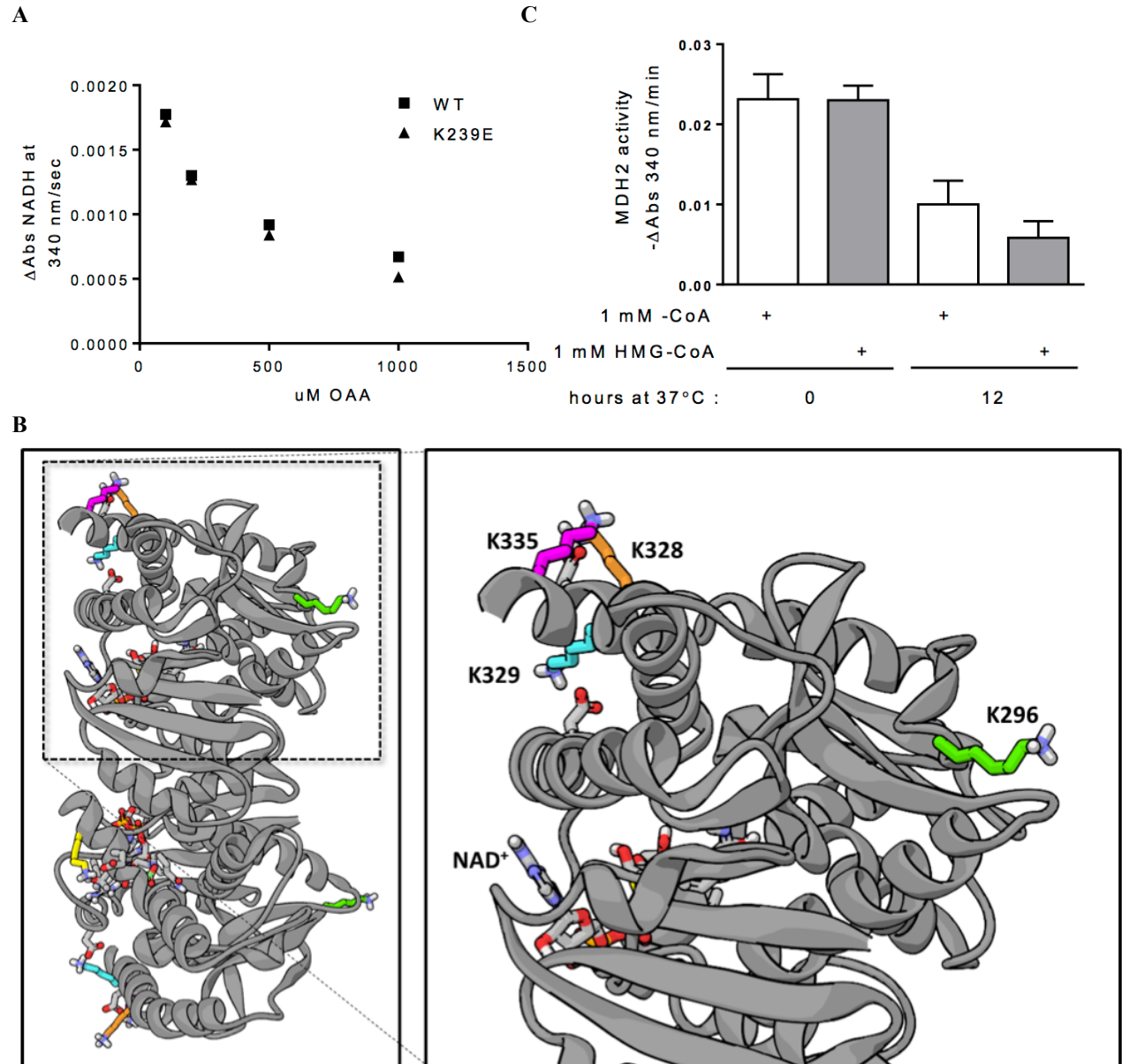


Figure S6, related to Figure 6.

(A) MDH2 exhibits substrate inhibition with increasing concentrations of oxaloacetate. Testing the effect of oxaloacetate concentration on the activity of WT human MDH2-myc and K239E constructs overexpressed in 293T cells. Due to substrate inhibition at higher concentrations, oxaloacetate was limited to $\leq 200 \mu\text{M}$ in the activity assays. See methods.

(B) MDH2 dimer showing location of lysine 296. Left panel shows the MDH2 dimer crystal structure modeling the HMGylated lysines at which glutamate mutations were made to mimic HMGylation and the right panel provides a closer image of those lysines in the monomer.

(C) MDH2 activity after exposure to CoA or HMG-CoA for 0 and 12 hours. Human recombinant MDH2 was incubated with 1 mM CoA or 1 mM HMG-CoA for 0 hours ($n=3$) or 12 hours ($n=4$ for +CoA, $n=5$ for +HMG-CoA). MDH2 activity in each sample was measured by monitoring the decrease in NADH absorbance as detailed in materials and methods. The right half of the graph (12 hrs) shown is primary Figure 6H. Data represent mean \pm standard deviation.